Supporting Information

Quoyer et al. 10.1073/pnas.1312515110

SI Materials and Methods

Plasmids. The plasmid encoding the G_1 subunit was bought at Missouri University of Science and Technology (cdna.org). The following plasmids were previously described: G_{i1}-91Rluc and $_{2A}$AR-YFP (1), GFP10-G_2 (2), CXCR4-Rluc and CXCR4-YFP (3), CXCR4-RlucII, CXCR4 5A tail-RlucII and GFP2–arrestin2 (4), RlucII-G_{13} and CXCR4-GFP_2 (5), -arrestin1-RlucII (6), GRK2-GFP2 (7). HA-CXCR4 and HA-CXCR4-YFP were cloned in pIRESP. The β-arrestin2-RlucII construct was built by replacing the GFP_{10}-EPAC sequence from the previously published GFP_{10}-EPAC-RlucII (6) with the coding sequence of human β-arrestin2. The human GRK3 cDNA was amplified by PCR and cloned in the pcDNA3.1 (+) RlucII-GFP10-strep tagx2 to substitute RlucII by the GRK fragment. The G_{i1}-91RlucII plasmid was constructed by replacing the Rluc on the G_{i1}-91Rluc (1) by RlucII. $G\alpha_{i2}$-RlucII and $G\alpha_{i3}$-RlucII were created using the same strategy as described in Richard-Lalonde et al (8) to generate the $G\alpha_oA99$-RlucII. The overlapping fragments were subcloned in the expression vector pcDNA3.1 zeo (+) (Invitrogen) and the resulting constructs encode for the corresponding human G alpha (i2 and i3) G protein subunit with an internal RlucII flanked by NAAIRS linkers in the loop connecting helices αA and αB of the helical domain.

Cell Culture and Transfections. Human Embryonic Kidney 293 (HEK293) T cells were cultured in Dulbecco's Modified Eagle's Medium (DMEM) supplemented with 5% (vol/vol) FBS, 100 Units of penicillin, 100 g/mL streptomycin and 2 mM L-glutamine. The day before transfections, cells were seeded in 6-well plates at a density of 600,000 cells/well. Transient transfections were performed using linear polyethyleimine 25 KDa (PEI, Polysciences, Inc.) as transfecting agent, at a ratio of 3 to 1 PEI / plasmid DNA (9). Culture medium was replaced with fresh medium 2 h after transfection. Cells were maintained in culture for the next 48 h, and BRET experiments carried out.

For stable cell lines, clonal cells were obtained by limited dilution. HEK293T cells stably expressing either -2-adaptin-eYFP (9) or obelin were maintained in DMEM supplemented with 10% (vol/vol) FBS, 100 Units of penicillin, 100 g/mL streptomycin and either 250 g/mL G418 or 100 g/mL hygromycin, respectively. SUP-T1 cells were maintained in RPMI-1640 supplemented with 10% (vol/vol) FBS, 100 Units of penicillin and 100 g/mL streptomycin.

Bioluminescence Resonance Energy Transfer Measurement. Two BRET configurations ($BRET_{480\text{-}YFP}$ and $BRET_{400\text{-}GFP2/10}$) were used in this study. For $BRET_{480\text{-}YFP}$ (previously termed $BRET^1$) (10), proteins were fused to Rluc or RlucII (a mutated brighter form of the Rluc; C124A/M185V-Rluc) and YFP as energy donors and acceptors, respectively. In this configuration, coelenterazine h (coel-h) (NanoLight Technology) was used as the luciferase substrate to generate light with a maximal emission peak at 480 nm. For $BRET_{400\text{-}GFP2}$ and $BRET_{400\text{-}GFP10}$ (previously termed $BRET^2$) (11), proteins were fused to Rluc or RlucII and GFP2 or GFP10 as energy donors and acceptors, respectively. The two variants of GFP can be excited at 400 nm and have almost identical emission spectra. In this configuration, coelenterazine 400a (coel-400a) (Biotium) was used as the luciferase substrate to generate light with a maximal emission peak at 400 nm. BRET was measured using a Mithras LB940 Multimode Microplate Reader (Berthold Technologies) equipped with either $BRET_{480\text{-}YFP}$ filter set (acceptor, 530 ± 20 nm; and donor, 480 ± 20 nm filters) or $BRET_{400\text{-}GFP2/10}$ filter set (acceptor, 515 ± 20 nm; and donor, 400 ± 70 nm filters).

For G protein engagement and G protein activation experiments, 2 d after transfection, cells were washed with Hank's Balanced Salt Solution (Invitrogen) supplemented with 20 mM Hepes (HBSS), detached, and resuspended in HBSS complemented with 0.1% BSA (HBSS/BSA) (Sigma-Aldrich) at room temperature. Then 100,000 cells per well were distributed in a 96-well microplate (Optiplate; PerkinElmer, Inc.). For β-arrestin and GRK recruitment experiments, cells were seeded the day after transfection in a Poly-L-ornithine (Sigma-Aldrich) pretreated 96-well microplate (CulturPlate; PerkinElmer, Inc). The day of the experiment, cells were incubated with HBSS/BSA, then treated with or without different concentrations of ligands for the indicated times. BRET values were collected following the addition of the luciferase substrate at a final concentration of 2.5 μM.

BRET signals were determined as the ratio of the light emitted by acceptors (YFP, GFP2, or GFP10) over donors (Rluc or RlucII). To determine the specific BRET signal (net BRET), the background signal detected in cells transfected with the luciferase donor alone was subtracted from the BRET values obtained in cells expressing the energy donor and acceptor. The ligand-promoted BRET signal (ΔBRET) was calculated by subtracting the BRET values obtained in the vehicle condition from the one measured with ligand.

BRET titration curves were performed by cotransfecting a constant amount of the donor with increasing amounts of the acceptor. BRET values were expressed as a function of the total expression level of the acceptor over the total expression level of the donor detected for each transfection condition.

Total Fluorescence and Luminescence Measurements. To determine the total expression level of the acceptor, total fluorescence was measured using a FluoroCount fluorometer (PerkinElmer, Inc.) with excitation filters at 485 or 400 nm and emission filters at 530 or 510 nm for YFP or GFP2/GFP10, respectively. To determine the total expression level of the donor, luminescence was measured using a Mithras LB940 Multimode Microplate Reader, following the addition of 2.5 μM coel-h or 2.5 μM coel-400a, respectively.

Western Blotting. Western blotting for CXCR4 pSer-324/5 and pSer-330 was performed as previously described (4). Briefly, HEK293 cells stably transfected with FLAG-tagged CXCR4 were cultured to 90% confluence in six-well plates. After a 6 h serum starvation, cells were incubated with 100 nM SDF-1 or 3 M ATI-2341 for 0-60 min. Cells were then lysed with ice-cold lysis buffer, and supernatants were separated on a 10% SDS/PAGE and incubated with 1:1,000 dilutions of anti-pSer-324/5 or pSer-330 CXCR4 antibodies followed by goat anti-rabbit Alexa Fluorophore 680-conjugated secondary antibody. Blots were visualized and analyzed using the ODYSSEY infrared imaging system.

Flow-Cytometry. Forty-eight hours after transfection with HA-CXCR4 or HA-CXCR4-Venus, HEK293T cells were rinsed with HBSS, resuspended in HBSS/BSA and incubated with SDF-1 or ATI-2341 for the indicated times. Cell surface receptors were labeled on ice using a monoclonal anti-HA antibody (HA-11; Covance) followed by an anti-mouse Alexa Fluor 647 secondary antibody (Invitrogen Canada).

SUP-T1 cells were resuspended in HBSS/BSA and stimulated with SDF-1 or ATI-2341 for 15 or 30 min. Cell surface CXCR4

were directly stained in HBSS containing Fc block solution 24G2 (anti-CD16/32-FcRγ) using an anti-human CXCR4 antibody [PerCP/Cy5.5 anti-human CD184 (CXCR4) antibody; BioLegend] for 45 min on ice.

Cells were washed, resuspended and analyzed through a LSR II flow-cytometer (BD Biosciences) set to detect YFP and Alexa Fluor 647 or PerCP/Cy5.5. Data analysis was performed using BD FACSDiva and FlowJo softwares.

Calcium Measurements. In HEK293T cells, obelin biosensor was used as a calcium reporter (12). HEK293T cells stably expressing obelin were incubated overnight in the presence or absence of 100 ng/mL PTX. Cells were then washed with HBSS, resuspended in HBSS/BSA, and incubated for 2 h in the dark, at room temperature, with 1 M coelenterazine cp (Biotium), the obelin substrate. Ligands were directly added in 96-well microplate (Optiplate) and 100,000 cells were then injected in each well using the SpectraMax L (Molecular Devices). Luminescence measurements were determined for each ligand concentration for 40 s. Full kinetics were normalized, setting the maximal response of carbachol at 100%. In SUP-T1 cells, calcium was measured using a calcium 4 dye. Cells were incubated overnight in the presence or absence of 100 ng/mL PTX. Cells were resuspended in HBSS/0.2% BSA and plated at 150,000 cells/well in 96-well clear bottom black plates (PerkinElmer). Calcium 4 dye (Molecular Devices) was then added before briefly centrifuging the plate to spin down the cells and incubating for 1 h at 37 °C. Compounds were then injected in the wells and calcium measurements were performed using the FlexStation II (Molecular Devices).

MAPK Experiments. For dose-response experiments, HEK293 cells stably expressing human CXCR4 were seeded in 96-well plates and were incubated overnight in serum-free medium in the presence or absence of 100 ng/mL PTX. Cells were stimulated with agonists for 5 min before lysis buffer was added. Cell lysates were transferred to 384-plate followed by detection reagents from Cellul'erk kit (Cisbio). TR-FRET signal was detected on a PHERAStar Plus (BMG). For kinetics experiments, HEK293T cells were seeded in 96-well plates and incubated overnight in DMEM supplemented with 0.1% BSA. Cells were stimulated with agonists for the indicated times and lysed overnight at –20 °C. Cell lysates were transferred into white 384-plate proxiplate plus (Perkin Elmer), incubated with both acceptor and donor beads from AlphaScreenSureFire kit (Perkin Elmer) at room temperature, and the phosphorylation of endogenous extracellular signal-regulated kinase 1 and 2 (ERK 1/2) was then determined using the multidetector plate reader FUSION (Packard Instrument Company).

Data and Statistical Analysis. All BRET data were analyzed using GraphPad Prism (GraphPad Software, Inc). Curves were fitted using least squares nonlinear regressions, assuming a one binding site hyperbola (for BRET titration curves), a sigmoidal fit (for dose-response curves), and a one-phase exponential decay or association curve (to calculate the half-life of kinetic experiments).

Bias factor of ATI-2341 for $G\alpha_i$ engagement versus the recruitment of β-arrestin2, GRK2, or GRK3 to CXCR4 was calculated by a method previously published by Kenakin et al. (13) using the "operational model" of Black and Leff (14). To calculate the bias, τ and K_A values were deduced from dose-response curves fitted using the operational model-partial agonist function. To calculate the $\Delta\text{Log}\,(\tau/K_A)$, which represents the relative ability of ATI-2341 to activate a given signaling pathway, we determined the $\text{Log}\,(\tau/K_A)$ values for each pathway and subtracted the $\text{Log}\,(\tau/K_A)$ for SDF-1 from the $\text{Log}\,(\tau/K_A)$ for ATI-2341. Finally, to determine the $\Delta\Delta\text{Log}\,(\tau/K_A)$, which represents the relative activity of ATI-2341 for a pathway toward another compared with SDF-1, the $\Delta\text{Log}\,(\tau/K_A)$ values calculated for each signaling pathway (β-arrestin2, GRK2 or GRK3 recruitment) were subtracted from the $\Delta\text{Log}\,(\tau/K_A)$ values calculated for the reference pathway ($G\alpha_i$ engagement). The bias factor is then determined as the anti-Log value of the $\Delta\Delta\text{Log}\,(\tau/K_A)$.

Statistical significance of the differences between two conditions was assessed using a Student *t* test whereas we used a one-way analysis of variance (ANOVA) followed by Bonferroni's multiple comparison test to assess statistically significant differences between multiple conditions. Differences yielding P values < 0.05 were considered as statistically significant.

1. Galés C, et al. (2006) Probing the activation-promoted structural rearrangements in preassembled receptor-G protein complexes. *Nat Struct Mol Biol* 13(9):778–786.
2. Galés C, et al. (2005) Real-time monitoring of receptor and G-protein interactions in living cells. *Nat Methods* 2(3):177–184.
3. Percherancier Y, et al. (2005) Bioluminescence resonance energy transfer reveals ligand-induced conformational changes in CXCR4 homo- and heterodimers. *J Biol Chem* 280(11):9895–9903.
4. Busillo JM, et al. (2010) Site-specific phosphorylation of CXCR4 is dynamically regulated by multiple kinases and results in differential modulation of CXCR4 signaling. *J Biol Chem* 285(10):7805–7817.
5. Yagi H, et al. (2011) A synthetic biology approach reveals a CXCR4-G13-Rho signaling axis driving transendothelial migration of metastatic breast cancer cells. *Sci Signal* 4(191):ra60.
6. Zimmerman B, et al. (2012) Differential β-arrestin-dependent conformational signaling and cellular responses revealed by angiotensin analogs. *Sci Signal* 5(221):ra33.
7. Breton B, Lagacé M, Bouvier M (2010) Combining resonance energy transfer methods reveals a complex between the alpha2A-adrenergic receptor, Galphai1beta1gamma2, and GRK2. *FASEB J* 24(12):4733–4743.
8. Richard-Lalonde M, et al. (2013) Conformational dynamics of Kir3.1/Kir3.2 channel activation via δ-opioid receptors. *Mol Pharmacol* 83(2):416–428.
9. Hamdan FF, et al. (2007) Unraveling G protein-coupled receptor endocytosis pathways using real-time monitoring of agonist-promoted interaction between beta-arrestins and AP-2. *J Biol Chem* 282(40):29089–29100.
10. Angers S, et al. (2000) Detection of beta 2-adrenergic receptor dimerization in living cells using bioluminescence resonance energy transfer (BRET). *Proc Natl Acad Sci USA* 97(7):3684–3689.
11. Mercier JF, Salahpour A, Angers S, Breit A, Bouvier M (2002) Quantitative assessment of beta 1- and beta 2-adrenergic receptor homo- and heterodimerization by bioluminescence resonance energy transfer. *J Biol Chem* 277(47):44925–44931.
12. Campbell AK, Dormer RL (1975) Studies on free calcium inside pigeon erythrocyte 'ghosts' by using the calcium-activated luminescent protein, obelin. *Biochem Soc Trans* 3(5):709–711.
13. Kenakin T, Watson C, Muniz-Medina V, Christopoulos A, Novick S (2012) A simple method for quantifying functional selectivity and agonist bias. *ACS Chem Neurosci* 3(3):193–203.
14. Black JW, Leff P (1983) Operational models of pharmacological agonism. *Proc R Soc Lond B Biol Sci* 220(1219):141–162.

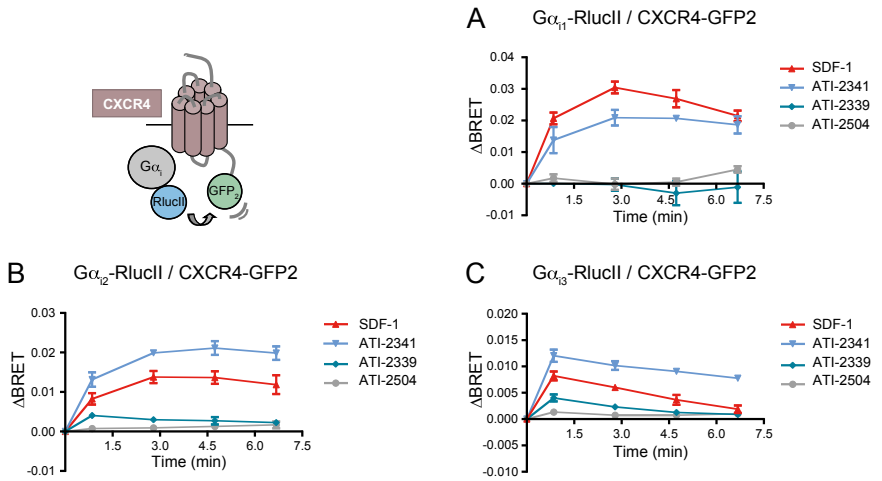

Fig. S1. ATI-2341 promotes the engagement of $G\alpha_{i1}$, $G\alpha_{i2}$, and $G\alpha_{i3}$. Kinetics of the ligand-promoted BRET between $G\alpha_{i1}$-RlucII (*A*), $G\alpha_{i2}$-RlucII (*B*), or $G\alpha_{i3}$-RlucII (*C*) and CXCR4-GFP2. BRET was measured after coel-400a addition, using the $BRET_{400\text{-}GFP2/10}$ filter set, at the indicated times following the addition of 200 nM SDF-1 or 1 μM pepducins (ATI-2341, 1 μM ATI-2339, and ATI-2504). As observed in $BRET_{480\text{-}YFP}$ configuration (Fig. 1*B*), the time-dependent engagement of $G\alpha_{i1}$ by the receptor was similar in $BRET_{400\text{-}GFP2}$ (*A*), suggesting that the results obtained are independent of the two BRET configurations used. SDF-1- and ATI-2341-promoted BRET increase between $G\alpha_{i2}$-RlucII (*B*) or $G\alpha_{i3}$-RlucII (*C*), and CXCR4-GFP2 showed a similar time-dependent engagement as the $G\alpha_{i1}$ protein subtype. Data shown are the mean ± SEM of three (*A* and *B*) or five (*C*) independent experiments.

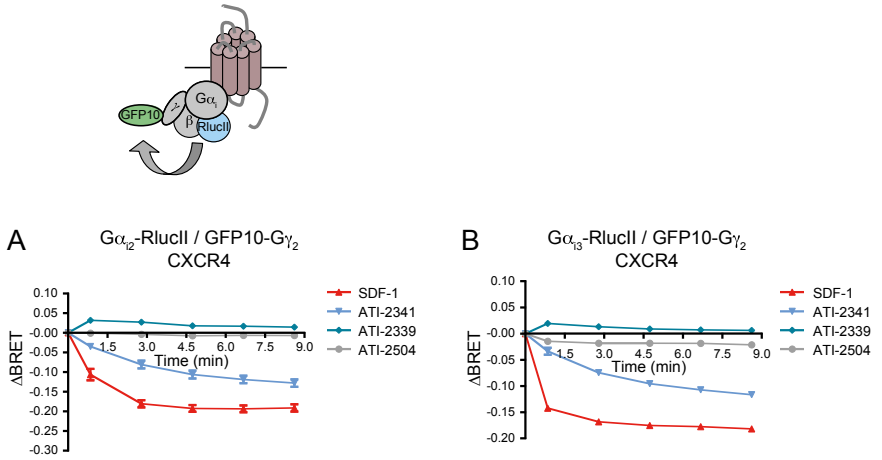

Fig. S2. ATI-2341-promoted $G\alpha_{i2}$ and $G\alpha_{i3}$ engagement results in their activation. Kinetics of the ligand-promoted BRET between $G\alpha_{i2}$-RlucII (*A*) or $G\alpha_{i3}$-RlucII (*B*) and GFP10-$G\gamma_2$ in cells cotransfected with the untagged Gβ subunit and CXCR4. BRET was measured after coel-400a addition, using the $BRET_{400\text{-}GFP2/10}$ filter set, at the indicated times following the addition of 500 nM SDF-1 or 1 μM pepducins (ATI-2341, 1 μM ATI-2339, and ATI-2504). The ATI-2341-activated CXCR4 also promoted G_{i2} and G_{i3} activation with similar kinetics as obtained for G_{i1}. Data shown are the mean ± SEM of four independent experiments.

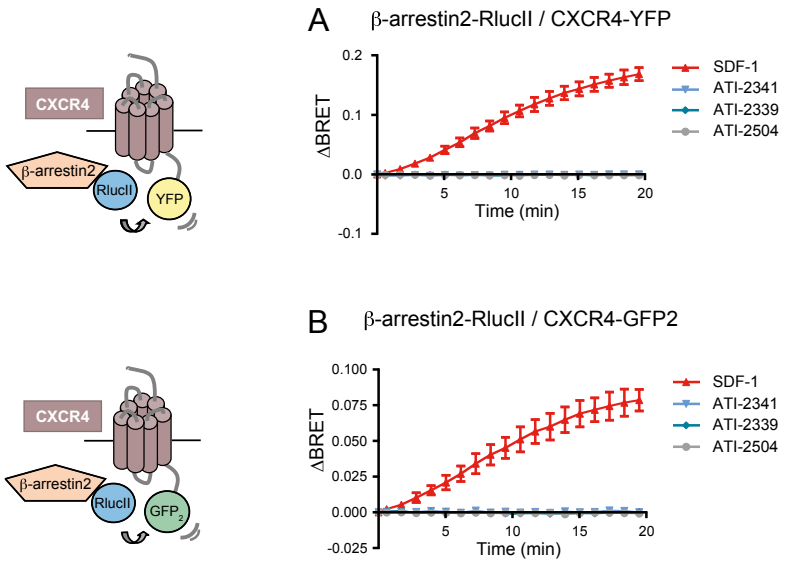

Fig. S3. The weak ATI-2341-promoted β-arrestin recruitment to CXCR4 is dependent neither of BRET orientation or BRET configuration. (*A*) Kinetics of the ligand-promoted BRET between β-arrestin2–RlucII and CXCR4-YFP. BRET was measured after coel-h addition, using the $BRET_{480\text{-}YFP}$ filter set, at the indicated times following the addition of 500 nM SDF-1 or 1 μM pepducins (ATI-2341, 1 μM ATI-2339, and ATI-2504). Data shown are the mean ± SEM of three independent experiments. (*B*) Kinetics of the ligand-promoted BRET between β-arrestin2–RlucII and CXCR4-GFP2. BRET was measured after coel-400a addition, using the $BRET_{400\text{-}GFP2/10}$ filter set, at the indicated times following the addition of 500 nM SDF-1 or 1 μM pepducins. Data shown are the mean ± SEM of three independent experiments. As previously observed in cells coexpressing CXCR4-RlucII and GFP2–β-arrestin2, ATI-2341 was unable to promote β-arrestin recruitment to CXCR4 in each BRET configuration or orientation used.

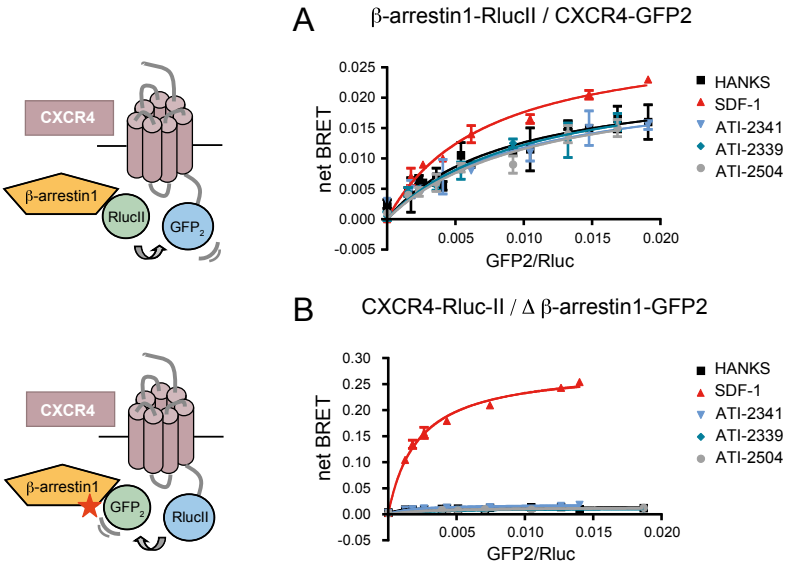

Fig. S4. ATI-2341 does not promote β-arrestin1 recruitment to CXCR4. BRET titration curves were performed in cells cotransfected with a constant amount of β-arrestin1–RlucII and increasing amounts of CXCR4-GFP2 (*A*) or in cells cotransfected with a constant amount of CXCR4-RlucII and increasing amounts of a truncated version of β-arrestin1–GFP2 (*B*). Cells were stimulated with 500 nM SDF-1, 1 μM pepducins (ATI-2341, 1 μM ATI-2339, and ATI-2504), or vehicle (Hanks) for 20 (*A*) or 10 (*B*) min. BRET was measured following coel-400a addition using the $BRET_{400\text{-}GFP2/10}$ filter set. The curves shown are derived from individual titration curves that are representative of three independent experiments. The error bars represent the mean ± SD from duplicate wells. As expected for a class A GPCR (1) such as CXCR4, the SDF-1–promoted recruitment of β-arrestin1 was much weaker than what was observed for β-arrestin2. To exclude that the lack of ATI-2341–promoted recruitment of β-arrestin1 may result from such reduced recruitment, we also tested a truncated mutant form of β-arrestin1 that yields much larger BRET signals upon SDF-1 stimulation. As was the case for the full-length β-arrestin1, ATI-2341 did not promote any BRET signal between β-arrestin1–GFP2 and CXCR4-RlucII despite a very large response for SDF-1.

1. Oakley RH, Laporte SA, Holt JA, Caron MG, Barak LS (2000) Differential affinities of visual arrestin, beta arrestin1, and beta arrestin2 for G protein-coupled receptors delineate two major classes of receptors. *J Biol Chem* 275(22):17201–17210.

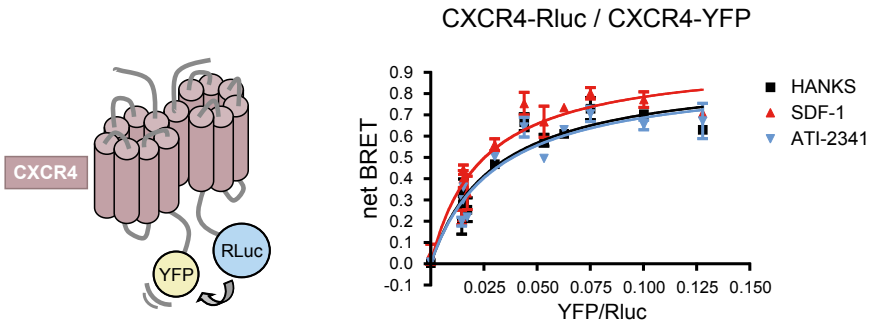

Fig. S5. ATI-2341 does not affect CXCR4 dimerization. BRET titration curves were performed in cells cotransfected with a constant amount of CXCR4-Rluc and increasing amounts of CXCR4-YFP. Cells were stimulated with 500 nM SDF-1, 1 μM ATI-2341, or vehicle for 20 min. BRET was measured following coel-h addition using the $BRET_{480\text{-}YFP}$ filter set. The curves shown are derived from individual titration curves that are representative of two independent experiments. The error bars represent the mean ± SD from duplicate wells. In contrast to SDF-1, which promotes an increase in BRET max, suggesting a conformational rearrangement within the dimer, ATI-2341 is without effect, suggesting that this pepducin does not affect CXCR4 dimerization.

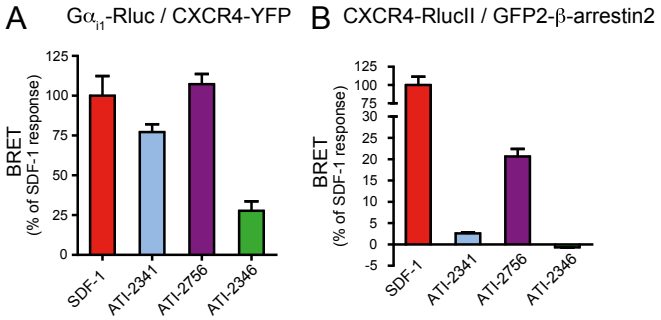

Fig. S6. (*A*) Ligand-promoted BRET between $G\alpha_{i1}$-Rluc and CXCR4-YFP. BRET was measured after coel-h addition, using the $BRET_{480\text{-}YFP}$ filter set following the addition of 500 nM SDF-1, 1 μM ATI-2341, 1 μM ATI-2756, or 1 μM ATI-2346 for 5 min. Data were normalized to SDF-1 response. Data are the mean ± SEM of three independent experiments. (*B*) Ligand-promoted BRET between CXCR4-RlucII and GFP2–β-arrestin2. BRET was measured after coel-400a addition, using the $BRET_{480\text{-}YFP}$ filter set following the addition of 500 nM SDF-1 or 1 μM pepducins for 10 min. Data were normalized to SDF-1 response. Data are the mean ± SEM of three independent experiments.

Table S1. Depiction of ATI-2341, ATI-2346, ATI-2756, ATI-2339, and ATI-2504 sequences

Pepducin	N-term	Sequence
ATI-2341	Pal	MGYQKKLRSMTDKYRL
ATI-2346	Pal	KKLRSMTDKYRLH
ATI-2756	Pal	GGYQKKLR p HTDKYRL
ATI-2339	Pal	MGYQKKLRSMTDK
ATI-2504		MGYQKKLRSMTDKYRL

Pepducins ATI-2341, ATI-2346, ATI-2756, and ATI-2339 with N-terminal (N-term) palmitate (Pal) are based on the sequence of the first intracellular loop region of the human CXCR4. ATI-2504 is an analog of ATI-2341 lacking the N-term palmitate moiety.